

AD-A090 351

ARMY ELECTRONICS RESEARCH AND DEVELOPMENT COMMAND FO--ETC F/G 9/1
SECOND HARMONIC GENERATION OF NEAR MILLIMETER WAVE RADIATION BY--ETC(U)
JUN 80 B H AMN, W W CLARK

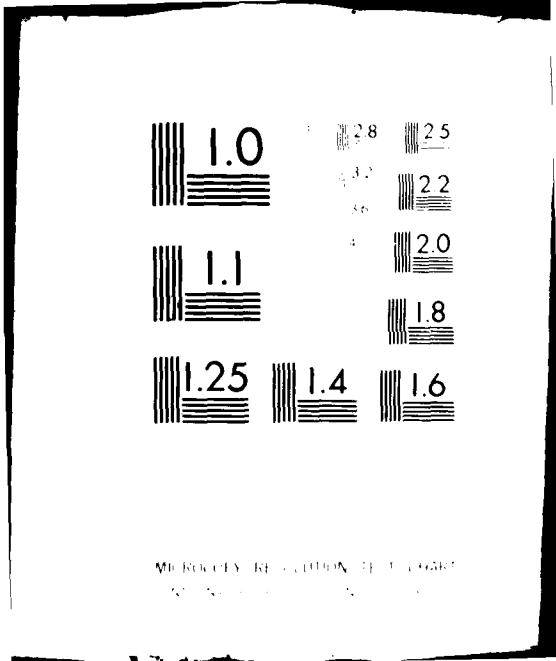
UNCLASSIFIED

NL

1 of 1
AD-A090 351



END
DATE
FILMED
11-80
DTIC



MEASUREMENT OF RESOLUTION
OF THE HUMAN EYE

*AHN & CLARK

11/11/80 (1)

(10) 15

AD A 090351

SECOND HARMONIC GENERATION OF NEAR MILLIMETER WAVE RADIATION BY NONLINEAR BULK MATERIAL. (U)

10 *BYONG H. AHN Mr.
WILLIAM W. CLARK, III PhD
NIGHT VISION & ELECTRO-OPTICS LABORATORY
FORT BELVOIR, VA 22060

JUN 1980

I. Introduction.

Bulk crystals have been used frequently to obtain second harmonic generation (SHG) and third harmonic generation (THG) of radiation from the fundamental input frequency, particularly in the optical region.

For example, ammonium dihydrogen phosphate, (1) potassium dihydrogen phosphate, (2) semiconductor materials, (3) and ferroelectric materials (4) were used for the SHG of input laser beams.

SHG and THG have also been realized in the microwave region. Boyd, et. al., (5) reported on the nonlinear coefficients and other important parameters at 55 GHz. Later, Boyd and Pollack (6) published a comprehensive paper on the nonlinear coefficients of LiTaO₃ and LiNbO₃ in the microwave region. DiDomenico, Jr., et. al., (7) obtained a 9 GHz TH output with an efficiency of 8.5% from a 2200 watt 3 GHz source by use of a 73% BaTiO₃ - 27% SrTiO₃ ceramic in a coaxial cavity configuration.

Impetus for bulk harmonic generation in the microwave region was given by the discovery that some ferroelectric (5) crystals have very large nonlinear coefficients, large enough to compensate for the lower frequencies of the microwave region in comparison to those of the optical region.

Our interest in SHG and THG in the microwave region started with the need for a radiation source at 220 GHz. Tube type sources

DDC FILE COPY

1

80 10 15 032
393741

*AHN & CLARK

(i.e., klystron and magnetron) and solid state sources (i.e., IMPATT and GUNN diodes) encounter inherent material limitations and fabrication difficulties in terms of the electron and hole mobility and the small geometrical dimensions and high electrical field. These problems make it difficult and/or impossible to obtain 220 GHz radiation from these sources. On the other hand, size and weight of the source are very important system design criteria. A powerful gyrotron is too big and too heavy a system for portable use. Extended Interaction Oscillators (EIO) represent recent source options whose specified output power is 60 W at 220 GHz. Unit cost, lifetime, and ease of fabrication are also important parameters for consideration. At the present time, the lower frequency radiation sources tend to have a longer lifetime and are easier to make, both of which result in lower cost.

After weighing various system parameters, such as the efficiency, weight, size, power output, lifetime, and ease of fabrication, it was decided to investigate the bulk SHG and THG techniques as an option to satisfy the requirement for source development for specific NV&EOL systems applications. The performance specifications of the EIO will be used as the basis for our requirements analysis.

This paper will develop the theoretical conversion efficiency equations for the SHG and THG, illustrate the input power requirements for the known nonlinear materials and the material requirements for the available input power sources, and list the ferroelectric materials which show promise as bulk crystal harmonic generators. The experimental setup and the preliminary results will be described briefly.

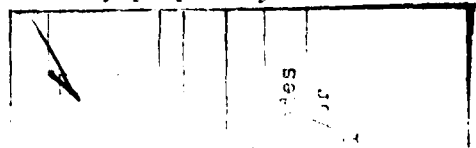
II. Theory.

1. SHG. SHG is possible only in acentric crystals, wherein the input radiation produces polarization at the second harmonic given by(8)

$$P_i(2\omega) = \epsilon_0 \sum_{j,k} d_{ijk}^m E_j(\omega) E_k(\omega) \quad \text{Eqn. (1)}$$

where $E_k(\omega)$ and $E_j(\omega)$ are the electric fields at the fundamental frequency, ω , ϵ_0 is the free space electric permittivity and d_{ijk}^m is the nonlinear coefficient.

a. Conversion Efficiency. Assuming the conversion efficiency is low and the absorption of the input power by the crystal is negligible, i.e., $E_{inc}^2(\omega)(z=0) \approx E_1^2(\omega)(z=l)$, then by proper adjustment



*AHN & CLARK

for d_{ijk}^m , the conversion efficiency can be expressed as (9)

$$\eta = p(2\omega)/p(\omega) = \frac{2\mu_0^{3/2}\epsilon_0^{1/2}\omega^2 (d^m)^2 \ell^2 p(\omega) \sin^2(\pi\ell/2\ell_c)}{n^3 A (\pi\ell/2\ell_c)^2} \quad \text{Eqn. (2)}$$

ℓ = interaction length
 A = beam size
 ℓ_c = coherence length
 n = index of refraction
 $p(\omega)$ = input power
 d^m = nonlinear coefficient, usually expressed in 10^{-12}m/V

unit.

The unit of d in Reference 9 is obtained by multiplying d^m in this paper by 8.85×10^{-12} . If the conversion efficiency is high, i.e., $E_{inc}^2(\omega)(z=0) = E_1^2(\omega)(z=\ell) + E_2^2(2\omega)(z=\ell)$, the conversion

efficiency is expressed as (10) $\eta = \tanh^2(\omega d^m E_{inc} \ell / nc)$

converting this to more familiar terms

$$\eta = \tanh^2[\sqrt{2} \omega d^m \epsilon_0 (\mu_0/\epsilon)^{3/4} \ell \sqrt{p(\omega)/A}] \quad \text{Eqn. (3)}$$

If the absorption is significant, then the second harmonic power is modified by (11) $p'(2\omega) = p(2\omega) \exp(-\alpha_\omega \ell + 1/2 \alpha_{2\omega} \ell)$

b. Nonlinear Coefficient. The generalized nonlinear coefficient is expressed as (12)

$$d^m(\omega) = \delta_{AB} [(\chi^i)^3 + (\chi^i)^2 (\chi^e)] + \delta_C (\chi^i) (\chi^e)^2 + \delta_D (\chi^e)^3 \quad \text{Eqn. (4)}$$

where χ^i = linear ionic susceptibility

χ^e = linear electronic susceptibility

$d^0 = \delta_D (\chi^e)^3$ nonlinear optical coefficient

the δ_i values in Eqn. (4) are all on the order of 10^{-12}m/V . In the optical region, only the linear electronic susceptibility χ^e contributes, whereas in the microwave region, all the terms contribute. In diatomic materials, such as GaAs and CdTe, χ^i is about the same as χ^e and d^m is about the same as d^0 . In ferroelectric materials, such as LiNbO_3 and BaTiO_3 , $\chi^i \gg \chi^e$ and $d^m \gg d^0$. Furthermore, the linear ionic susceptibility is related to the electrical permittivity as $\chi^i = \epsilon/\epsilon_0 - n^2 - 1$ and $\chi^e = n^2 - 1$ (this n is the index of

refraction in the optical region). This indicates that a promising nonlinear material in the microwave region will have a large electrical permittivity, ϵ . In the ferroelectric crystals where $\chi^i \gg \chi^e$, we can assume that $\chi^i \approx \epsilon_\omega / \epsilon_0 = n_\omega^2$, where ϵ_ω is the microwave electrical permittivity. The magnitude of the microwave nonlinear coefficient can be approximated as $d^m \approx \delta_{AB} (\chi^i)^3$

$$\approx \delta_{AB} (\epsilon_\omega / \epsilon_0)^3 \quad \text{Eqn. (5)}$$

$$\approx \delta_{AB} (n_\omega)^6$$

In the conversion efficiency, Eqn. (2), we notice that $\eta \propto (d^m)^2 / n^3$. By use of Eqn. (5), the above relationship can be expressed as

$$\eta \propto \delta_{AB}^2 (n_\omega^m)^{12} / (n_\omega^m)^3$$

$$\eta \propto (\delta_{AB})^2 n_\omega^9 \quad \text{Eqn. (6)}$$

The conversion efficiency is thus proportional to the 9th power of the index of the refraction in the microwave region.

The following table gives the summary of important parameters for SHG in bulk crystals.

Table I. Physical Parameters of Bulk Harmonic Generators⁽⁵⁾

MATERIAL	POINT GROUP	n_e	ϵ / ϵ_0	α cm ⁻¹	χ^e	χ^i	δ_{AB} 10 ⁻¹² m/V	d_{ijk} 10 ⁻¹² m/V	ijk
BaTiO ₃	4mm	2.29	57	1.7	4.25	52	0.64	97,000	333
LiTaO ₃	3m	2.14	40	1.0	3.58	35.4	0.33	16,000	333
LiNbO ₃	3m	2.16	25.5	0.5	3.66	20.8	0.63	6,700	333
KDP*	$\bar{4}2m$	1.51	44	0.9	1.24	41.8	0.053	1,850	123
		1.47	21		1.13	18.9			
GaAs	$\bar{4}3m$	3.27	13.05	0.024	9.71	2.34	+0.12 -1.40	±51	123

*Upper and lower values are for 1- and 3- axes, respectively.

Pollack and Turner⁽¹³⁾ reported the magnitude of BaTiO₃ in d_{113}^m to be $+3.9 \times 10^7$ in the units of 10^{-12}m/V . This value is greater than d_{33}^m of BaTiO₃ by a factor of 402. This is largely due to the constant strain dielectric constant of BaTiO₃ in the 1-axis, which is 2300.

c. Discussion. The coherence length in Eqn. (2) is the maximum useful length of the crystal for SHG.

In the optical region, the coherence length can be made large by carefully orienting the birefringent crystal such that $n_{2\omega}$ is very nearly equal to n_{ω} in the direction of the respective radiations. No such precaution is used in the microwave region because of the longer wavelength. Letting $n_{2\omega} - n_{\omega} = 0.01$,⁽¹⁴⁾ l_c at $\lambda = 5.45 \text{mm}$ (55 GHz) is 136mm.

Other factors which affect the conversion efficiency are the frequency, nonlinear coefficient, index of refraction, and the beam size. The decrease in frequency in going from the optical to the NMMW region is offset by the increase in the nonlinear coefficient, d^m , as can be seen in Table I. However, the increase in conversion efficiency due to the material coefficients is reduced somewhat by the factor of n^3 in the denominator of Eqn. (2). The true material dependence is given by Eqn. (6) which shows that conversion efficiency is roughly proportional to n^9 .

The conversion efficiency is also affected by the decrease in radiation intensity in the NMMW region. Assuming the beam size is limited by diffraction, the intensity is proportional to the inverse square of the wavelength. In going from a wavelength of $1 \mu\text{m}$ to 1mm the reduction in conversion efficiency is on the order of 10^6 . The beam size in the NMMW region can be made somewhat smaller by use of waveguide.

2. Third Harmonic Generation (THG). THG is another technique to use for frequency multiplication. Cubic crystals can be used for THG. Terhune, et. al.,⁽¹⁵⁾ obtained THG from calcite using a ruby laser with a peak power of 200 kW. The conversion efficiency obtained was about 4×10^{-6} . Shelton and Shen⁽¹⁶⁾ obtained THG in cholesteric liquid crystals. Puell and Vidal⁽¹⁷⁾ obtained THG from alkali metal vapors. Akitt and Coleman⁽¹⁸⁾ obtained THG in HCN gas in the microwave region with an efficiency of 1.5×10^{-5} using a 100 kW source. Bloom, et. al.,⁽¹⁹⁾ obtained a high conversion efficiency of 10% in a medium of xenon and rubidium with a mode-locked Nd:YAG laser with a peak power of 3×10^8 watt. Depending upon the available input power, THG can be a viable option to SHG.

*AHN & CLARK

The induced third-order polarization is given by

$$p^{(3)}(3\omega) = \epsilon_0 \chi^{(3)} E^3(\omega)$$

and the third harmonic output by (20)

$$p^{(3)}(3\omega) = \frac{9\mu_0^2 \omega^2 \ell^2 (\chi^{(3)})^2 p^3(\omega) \sin^2(\pi \ell / 2 \ell_c)}{n A^2 (\pi \ell / 2 \ell_c)^2}$$

where $\ell_c = \lambda / 6(n_{3\omega} - n_\omega)$

It can be seen that the third harmonic output is proportional to the third power of the input signal strength. The third harmonic nonlinear coefficients are typically smaller by a factor of 10^5 - 10^8 from their second harmonic counterparts. SrTiO_3 is an example of a material with a high nonlinear third harmonic coefficient in the NMMW region.

3. Temperature Effects. Changing the temperature can affect the SHG or THG in a number of ways. For instance, the phase transition temperature determines the crystal symmetry and thus its harmonic application. Theoretically SHG is possible only in acentric crystals.

Ferroelectric crystals have cubic symmetry in the paraelectric phase, cubic perovskite. In their ferroelectric phase, below the phase transition temperature, they lose the center of inversion. For example, KTaO_3 has a cubic symmetry at room temperature, but was observed to generate SH and TH at 4.2 K, (21) a few degrees above the extrapolated Curie temperature. The conversion efficiency for SHG was 10^{-3} - 10^{-4} and for THG was 10^{-5} - 10^{-6} in the 2-5 GHz range. Another example is SrTiO_3 which goes from cubic to tetragonal (C_{4v}) below 100 K. (22)

The index of refraction and the absorption coefficient also depend upon the temperature as well as the frequency. (14) Both values are smaller at the lower temperature and longer wavelengths. In addition, dielectric constants undergo a dramatic change around the Curie temperature (23) and follow the Curie-Weiss law for ferroelectric crystals.

Kaminov and Harding (24) measured the change in the dielectric constant and the loss tangent as a function of temperature at 9.2 GHz in KDP ($T_c = 123^\circ\text{K}$) and Talyanskjii, et. al., (25) found that in general the second harmonic and the nonlinear coefficient changed in the same manner as the dielectric constants. They found that the

*AHN & CLARK

SH power at -120°C goes up as much as 7.5 times the room temperature SH power.

4. Applied DC Fields. Symmetric crystals can also be distorted into acentric structures under the influence of electric fields. Calcite, which possesses a center of inversion, was observed to generate SH even without an applied field. (26, 27) The output was observed to increase by a factor of 10 in a dc field of 200 kV/cm. The effective nonlinear coefficient in the optical region was about $3 \times 10^{-4} d_{36}$ (ADP). Maker and Terhune (20) expressed the nonlinear polarization of the electric field induced SHG in calcite by

$$p^{(3)}(3\omega) = 2\epsilon_0 \chi^{(3)} E^2(\omega) E_{dc}$$

They reported that with $E_{dc} = 20$ kV/cm, SH power was about 1/500 that of KDP under similar setup using a ruby laser.

In SrTiO_3 the transverse optical frequency (ω_{TO}) at 8 K shifts from 10 cm^{-1} to 45 cm^{-1} with an applied field of 12 kV/cm. (9) It is also slightly deformed under the dc field by about .056%. (28) This material can be grown by the flame fusion techniques in large sizes (1x1x2 cm).

5. Numerical Calculation of the Output Power. Using the conversion efficiency equation, the SH power of LiNbO_3 , LiTaO_3 , and BaTiO_3 is calculated using an input power of .1 W at 55 GHz with a sample length of 1 cm.

LiNbO_3	$P(2\omega) = .049 \times 10^{-9} \text{ W}$
LiTaO_3	$P(2\omega) = .14 \times 10^{-9} \text{ W}$
BaTiO_3	$P(2\omega) = 3.35 \times 10^{-9} \text{ W}$

The above numbers assume that the input beam fills the waveguide, the phase is matched, and the polarization of the beam and the crystal orientation are consistent with the nonlinear coefficients given in Table I. It can be seen that at this input power level (which is typical for a klystron oscillator) a very sensitive detector is necessary to observe the SH output.

6. Performance Criteria for the Harmonic Generation. For high SHG, we must have a crystal with high d^m and/or a high power fundamental source.

An EIO producing 1 kW at 110 GHz and 60 W at 220 GHz is available from Varian of Canada. An equivalent conversion efficiency of 6% is used as the performance baseline.

*AHN & CLARK

By use of a BaTiO_3 crystal 1 cm long (d_{333}^m) and an EIO of 1 KW at 110 GHz, a calculated SH output of 4.46 W ($\eta=.446\%$) is obtained. Using the same crystal in the d_{113}^m mode a SH output of 174 W should be obtained.

For THG, SrTiO_3 requires a fundamental input power of 150 megawatts to obtain a 100 W third harmonic output at 210 GHz (assuming a value $\chi^{(3)}=7 \times 10^{-19}$ (mks) from optical data).

7. Crystals with High SHG Possibility. Ferroelectric crystals above and below the phase transition temperature can be useful for THG and SHG respectively in the microwave region. This is mainly due to the large ionic linear susceptibility which is related to the crystal distortion from the cubic structure. The materials with non-cubic structure and high constant-strain dielectric constants are selected for further study.

$\text{K}_6\text{Li}_4\text{NbO}_3$, (29) a crystal symmetry of 4mm, has a Curie temperature of 420°C and was found to be stable under high laser intensity. Its constant-strain dielectric constant is approximately 295 at 100 MHz. This material showed nonlinear properties comparable to LiNbO_3 without double refraction in the optical region. The ratio of K and Li can be changed to obtain different physical parameters.

$\text{Sr}_x\text{Ba}_{1-x}\text{Nb}_2\text{O}_6$, (30) 4mm, is another ferroelectric which shows promise as a SHG material in the NMMW. Depending upon the mix of Sr and Ba, the Curie temperature is found to vary between 60°C to 250°C and the dielectric constant varies from 118 to 3400 (measured at 15 MHz).

$\text{KSr}_2\text{Nb}_5\text{O}_{15}$ (31) has a tetragonal crystal symmetry with a Curie temperature of +160°C and a dielectric constant of 10^3 at 10^4 Hz. It was grown by the Czochralski technique and, again, its physical parameters can be varied by the K-Sr mix.

III. Experiment.

1. SHG and THG. Figure 1 shows the experimental arrangement for SHG and THG.

*AHN & CLARK

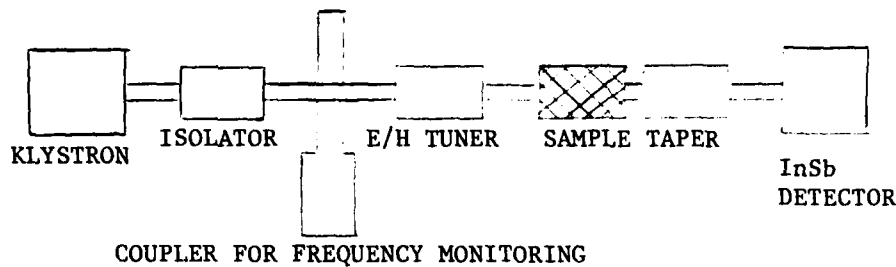


Figure 1. Experimental Setup

Fundamental power from a klystron is sent through various monitoring and tuning devices and then onto the sample which is inserted in fundamental waveguide. For observation of the SH the signal from the sample passes through a waveguide taper section which attenuates the fundamental frequency. The remaining signal is sent into a cooled InSb detector. For observation of the fundamental frequency the taper section is eliminated. For temperature effect measurements E - bend waveguide sections can be placed before and after the sample to enable it to be placed into a cooled bath at various temperatures.

For dc field studies, a slotted waveguide section was used such that the crystal could be inserted directly into the waveguide through the top (broad face). For this experiment, the crystal was coated with conducting paste on the top and bottom, and the high voltage lead could be passed through the slot in the waveguide and soldered to the crystal. The ground lead was connected to the waveguide.

A quasi-optical arrangement can also be used in which the output from the E/H tuner is radiated into the open air with a gain horn. This radiation is focused onto the sample by TPX lenses. The output from the sample is collected by the appropriate gain horn and waveguide system to filter out the fundamental frequency power.

2. d^m Measurement. (3) The nonlinear coefficient is determined by measuring the side-band power and the carrier power when the crystal is modulated by an a-c field above the piezoelectric resonance frequency. The sideband-to-carrier power ratio is approximately (4)

$$\frac{p(\omega_3)}{p(\omega_2)} \approx \frac{\omega_3^2 (d_{\text{eff}}^m)^2 (\ell/b)^2 v(\omega_1)^2}{c^2 \epsilon_3 / \epsilon_0}$$

*AHN & CLARK

where b is the width of the waveguide
 $V(\omega_1)$ is the modulating voltage
 ω_2 is the carrier frequency
 ω_3 is the sideband frequency

The experimental apparatus is similar to that used to study the dc effects.

3. Experimental Results and Analysis. The experiment was performed at 55 GHz using an OKI klystron with an output of about 0.1 watt. There was also the klystron generated second harmonic (KGS2) and third harmonic which had to be considered in the measurements. The low power measurements were made by using the manufacturers responsivity specifications of 3910 V/W for the InSb detector.

The results obtained should be considered as preliminary and qualitative. There were uncertainties as to the true temperature of the sample crystal with respect to the temperature of the waveguide which was monitored with a copper-constantin thermocouple and a digital voltmeter. The thermocouple was soldered to the waveguide adjacent to the sample crystal. The temperature of the waveguide and the sample were varied with LN₂ and a heat gun; no attempt was made to keep the sample crystal at a particular temperature other than at LN₂ temperatures and room temperature.

As the crystals were cooled the output fluctuated as much as an order of magnitude. This may be due to resonance behavior of the cavity formed by the crystals in the waveguide where the resonant frequency changes with temperature variations of the crystal index of refraction. In such cases the transmission should show maxima at ⁽¹³⁾ $K\ell = I\pi$ and minima at $K\ell = (I+1/2)\pi$ where K is the propagation constant in the crystal and I is an integer.

Measurements on the transmission and fluctuation of the fundamental frequency signal were made to explain the results obtained with the second harmonic frequency signal. For example, the change in the absorption coefficient at the second harmonic between 300 K and 77 K was assumed to be the same as that observed at the fundamental frequency.

a. Fundamental Frequency. Observation of the fundamental frequency signal produced two phenomena:

i) There were variations in the output power which may be due to crystal cavity resonance. Upon cooling a 22mm sample of LiNbO₃ produced the same number of maxima and minima in transmission as

*AHN & CLARK

predicted. But in samples of LiTaO_3 there were more maxima and minima than predicted assuming that the index of refraction changes the same as LiNbO_3 ($\Delta n \approx .2$).⁽¹⁴⁾ The discrepancy was not rectified when thermal expansion was considered, and is still open to discussion.

ii) The absorption coefficient of LiTaO_3 was reduced 0.9 cm^{-1} upon cooling from 300 to 77 K. The absorption coefficient of LiNbO_3 was found to be 2.64 cm^{-1} and did not change appreciably between 300 K and 77 K. This value is 5 times higher than previously reported.

b. Second Harmonic. As mentioned earlier, the klystron was observed to generate a second harmonic signal of its own, as much as $140 \times 10^{-10} \text{ W}$, which was significant compared to the calculated bulk crystal SH as shown in Table II. This 110 GHz input to the crystal had to be accounted for in the total SH output. But this signal was attenuated completely at room temperature by all the samples except a 0.5 cm LiNbO_3 . As the samples were cooled, the amplitude of the 110 GHz signal increased. The magnitudes of the 110 GHz signals at liquid nitrogen temperatures are also shown in Table II.

Table II. Effect of Temperature in the Second Harmonic Signal

MATERIAL	LENGTH	CALCULATED SH SIGNAL (300°K)	EXPERIMENTAL* SH SIGNAL (300°K)	EXPERIMENTAL SH SIGNAL (77°K)
LiNbO_3	2.2cm	2.4×10^{-10} watts	no signal	$5-10 \times 10^{-10}$
	0.5cm	0.1×10^{-10} watts	$\sim 1 \times 10^{-10}$ watts	$2.5-5 \times 10^{-10}$ watts
LiTaO_3	0.775cm	0.8×10^{-10} watts	no signal	3.1×10^{-10} watts
	1.0cm	1.4×10^{-10} watts	no signal	7.3×10^{-10} watts

*Detection limit is of the order of 1×10^{-10} watts.

*AHN & CLARK

As can be seen, the SH frequency signal increased in each case upon lowering the temperature. Two explanations are provided:

i) Increase in transmission of the klystron SH. This should not account for more than 2×10^{-10} watts assuming that the absorption coefficient at the SH frequency behaves similarly to the observed absorption coefficient at the fundamental frequency.

ii) Increase in the crystal generated SH due to the increase in the fundamental frequency input caused by the reduction of the absorption. This increases the SH power by the square of the increase in the input power (see Eqn. (2)). This amounts to an increase by a factor of 4. On the other hand, the SH signal is also proportional to the 9th power of the index of refraction. This reduces the bulk generated SH by 25%-30% assuming the index of refraction decreases by 0.2.⁽¹⁴⁾ The net gain in the bulk generated SH is, therefore, a factor of 3. If the calculated SH signals in Table II are multiplied by a factor of 3, they are comparable to the experimental values except in the 0.5cm LiNbO_3 .

There was some indication of resonance behavior in LiNbO_3 at 110 GHz but none was seen in LiTaO_3 .

SrTiO_3 and proustite were also tested at 110 GHz but no signal or change in the signal amplitude was detected even with cooling. In KDP a signal was observed upon cooling but no absolute measurements were made.

IV. Conclusion.

The review was made on the need, the theory, the techniques, and the materials suitable for the SHG and THG. Further research on materials in forms of the growth technique and the characterization of physical parameters is needed.

Some of the important features of these are:

- i) Large size availability.
- ii) Large linear ionic susceptibility.
- iii) High microwave intensity damage threshold.
- iv) Proper crystal symmetry.

*AHN & CLARK

The materials with high potential are $K_xLi_{1-x}NbO_3$, $Sr_xBa_{1-x}Nb_2O_6$, and $K_xSr_{1-x}Nb_5O_{15}$. The potential payoff is a 220 GHz source which has a longer lifetime, is easy to fabricate, and is readily available.

Preliminary results were also reported and analyzed. It was observed that the cavity resonance behavior makes the crystal length and the possible location of the sample in the waveguide important parameters of experiment. The increased signal strength of the harmonic frequency at lower temperatures cannot be explained by the reduction of the absorption coefficient alone. More efficient transmission of the fundamental input with consequent increase in the bulk generated SH could have contributed to the result. Further experiments will be done to verify the result.

The authors gratefully acknowledge Professor F. DeLucia of Duke University for many valuable technical discussions and for the use of the Duke University Microwave Laboratory equipments and facilities.

*AHN & CLARK

References.

1. N.I. Adams and P.B. Schoefer, Appl. Phys. Lett. 3, 19, (1963).
2. J.A. Giordmaine, Phys. Rev. Lett. 8, 19 (1962).
3. R.C. Miller, Appl. Phys. Lett. 5, 17, (1964).
4. G.D. Boyd, R.C. Miller, K. Nassau, W.L. Bond, and A. Savage, Appl. Phys. Lett. 5, 234 (1964).
5. G.D. Boyd, T.J. Bridges, M.A. Pollack, and E.H. Turner, Phys. Rev. Lett. 26, 387 (1971).
6. G.D. Boyd and M.A. Pollack, Phys. Rev. B 7, 5345 (1973).
7. M. DiDomenico, Jr., D.A. Johnson, and R.H. Pantell, J. Appl. Phys. 33, 1697 (1962).
8. J.G. Bergman and S.K. Kurtz, Mater. Sci. Eng. 5, 235 (1969/70).
9. A. Yariv, Introduction to Optical Electronics, 2nd Ed., Holt, Rinehart and Winston, 1976.
10. R.L. Byer and R.L. Herbst, Nonlinear Infrared Generation, ed Y.R. Shen, P. 87, Springer-Verlag, 1977.
11. S. Singh, Handbook of Lasers, P. 496, The Chemical Rubber Company, Cleveland, OH.
12. C.G.B. Garrett, IEEE J. Quantum Electronics 4, 70 (1968).
13. M.A. Pollack and E.H. Turner, Phys. Rev. B 4, 4578 (1971).
14. D.R. Bosomworth, Appl. Phys. Lett. 9, 330 (1966).
15. R.W. Terhune, P.D. Maker and C.M. Savage, Appl. Phys. Lett. 2, 54 (1963).
16. J.W. Shelton and Y.R. Shen, Phys. Rev. Lett. 25, 23 (1970).
17. H.B. Puell and C.R. Vidal, IEEE J. Quantum Electronics 14, 364 (1978).
18. D.P. Akitt and P.D. Coleman, J. Appl. Phys. 36, 2004 (1965).

*AHN & CLARK

19. D.M. Bloom, G.W. Bekkers, J.F. Young and S.E. Harris, Appl. Phys. Lett. 26, 687 (1975).
20. P.D. Maker and R.W. Terhune, Phys. Rev., V 137, A801 (1965).
21. J.E. Geusic, S.K. Kurtz, T.J. Nelson and S.H. Wemple, Appl. Phys. Lett. 2, 185 (1963).
22. R.C. Casella, Phys. Rev., V 154, 743 (1967).
23. C. Kittel, Introduction to Solid State Physics, 2nd Ed., John Wiley and Sons, Inc. (1956).
24. I.P. Kaminow and G.O. Harding, Phys. Rev., V 129, 1562 (1963).
25. V.I. Talyanskii, A.A. Filimonov and E.G. Yashchin, Sov. Phys. Solid St. 12, 2224 (1971).
26. R.W. Terhune, P.D. Maker and C.M. Savage, Phys. Rev. Lett. 8, 404 (1962).
27. J.E. Bjorkholm and A.E. Siegman, Phys. Rev., V 154, 851 (1967).
28. Lytle, J. Appl. Phys. 35, 2212 (1964).
29. L.G. Van Uitert, S. Singh, H.J. Levinstein, J.E. Geusic and W.A. Bonner, Appl. Phys. Lett. 11, 169 (1967).
30. P.V. Lenzo, E.G. Spenur, A.A. Ballman, Appl. Phys. Lett. 11, 23 (1967).
31. E.A. Giess, G. Burns, D.F. O'Kane and A.W. Smith, Appl. Phys. Lett. 11, 233 (1967).

(43)